

A&A manuscript no.

(will be inserted by hand later)

Your thesaurus codes are:

03(13.25.2; 11.01.2; 11.19.1; 11.09.1 IRAS12393+3520; 11.09.4; 11.14.1)

ASTRONOMY  
AND  
ASTROPHYSICS

# A direct view of the AGN powering IRAS12393+3520

M. Guainazzi<sup>1,2</sup>, M. Dennefeld<sup>3\*</sup>, L. Piro<sup>4</sup>, T. Boller<sup>5</sup>, P. Rafanelli<sup>6</sup>, M. Yamauchi<sup>7</sup>

<sup>1</sup> Astrophysics Division, Space Science Department of ESA, ESTEC, Postbus 299, NL-2200 AG Noordwijk, The Netherlands

<sup>2</sup> XMM SOC, VILSPA, ESA, Apartado 50727, E-28080 Madrid, Spain

<sup>3</sup> Institut d'Astrophysique de Paris, 98bis Bd Arago, F-75014 Paris, France

<sup>4</sup> Istituto di Astrofisica Spaziale, CNR, Via Fosso del Cavaliere, I-00131 Roma, Italy

<sup>5</sup> Max-Planck Institut for Extraterrestrial Physics, D-85740 Garching, Germany

<sup>6</sup> Università degli Studi di Padova, Dipartimento di Astronomia, Vicolo dell'Osservatorio 5, I-35122 Padova, Italy

<sup>7</sup> Astrophysics Laboratory, Dept. of Applied Physics, Faculty of Engineering, Miyazaki University, 1-1 Gakuen-Kibandai-Nishi, Miyazaki 889-2192, Japan

Received 10 November 1999 ; accepted 21 December 1999

**Abstract.** We report the first direct X-ray evidence that an AGN is hidden in the center of IRAS12393+3520. An ASCA observation of this target unveiled a bright (0.5–10 keV luminosity  $3.9 \times 10^{42}$  erg s<sup>-1</sup>) and variable source, with minimum observed doubling/halving time scale comprised in the range 30–75 ks. A model composed by a simple power-law, with photon index  $\simeq 1.8$  and an absorption edge, whose threshold energy is consistent with K-shell photoionization of OVII, provides an adequate fit of the spectrum. This suggests that we are observing the emission from the nuclear region through a warm absorber of  $N_{\text{H}} \simeq$  a few  $10^{21}$  cm<sup>-2</sup>. If it has internal dust with Galactic gas-to-dust ratio, it could explain the lack of broad H $\beta$  emission, even in the episodic presence of a broad H $\alpha$  emission line. Optical spectra obtained over several years show indeed variations in the strength of this broad H $\alpha$  component. A distribution of dusty, optically thick matter on spatial scales a few hundreds parsec, which does *not* intercept the line of sight towards the nucleus, is probably required to account simultaneously for the relative [OIII] luminosity deficit in comparison to the X-rays. The high IR to X-ray luminosity ratio is most likely due to intense star formation in the circumnuclear region. IRAS12393+3520 might thus exhibit simultaneously nuclear activity *and* remarkable star formation.

**Key words:** X-rays: galaxies – Galaxies: active – Galaxies: Seyfert – Galaxies: individual: IRAS12393+3520 – Galaxies: ISM – Galaxies: nuclei

Send offprint requests to: M. Guainazzi,  
mguainaz@xmm.vilspa.esa.es

\* Visiting astronomer, Observatoire de Haute-Provence (OHP), CNRS, France

## 1. Introduction

The correlation between the ROSAT All Sky Survey (RASS) and the IRAS Point Source Catalog unveiled the existence of many galaxies with X-ray luminosity in the range  $10^{42}$ – $10^{43}$  erg s<sup>-1</sup>, which had not been previously classified as Active Galactic Nuclei (AGN) (Boller et al. 1992). Subsequent optical observations indicated that a large fraction of them were previously unrecognized Seyfert galaxies (Moran et al. 1994, 1996; Dennefeld et al. in preparation). However, the nature of a few of them is far from being understood in terms of simple nuclear activity and deserves further investigations. IRAS12393+3520 (NGC 4619) is one of those, which we started to study in more details in 1992.

It is a nearby ( $z = 0.023$ ) barred spiral galaxy of morphological type SB(r)b, with a luminous nucleus and relatively weak spiral arms. Our first optical spectrum (Boller et al. 1993) was obtained at low resolution in March 1992 at the 1.93m telescope of Haute-Provence Observatory (OHP) and is displayed in Fig. 1. It shows a red continuum, typical of IRAS galaxies, with many stellar absorption features and conspicuous emission only in the red part of the spectrum (H $\alpha$ , [NII]). H $\beta$  is in absorption, and the [OIII] emission barely visible. The existence of a strong NaD absorption line is an indication that significant internal extinction is present. No clear evidence is seen of a broad H $\alpha$  component: a hint of it may be seen on the red side of the narrow emission line, but the presence of the atmospheric B band does not allow a proper estimate of the level of the continuum; this prompted further observations.

In the mean time, other spectra were published by Moran et al. (1994) and Mas-Hesse et al. (1996, hereinafter M96), showing a broad H $\alpha$  component attributed to a Seyfert 1 nucleus. While their two low-dispersion spectra are compatible with each other, their strong, broad H $\alpha$  line is not seen on ours. A high-resolution spectrum

arXiv:astro-ph/0001371v1 21 Jan 2000

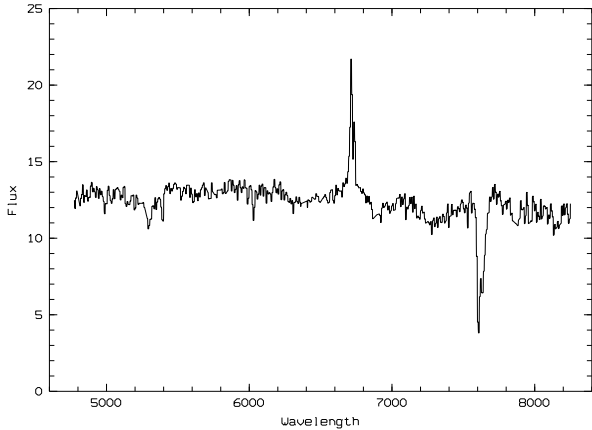


**Fig. 1.** March 1992 low resolution spectrum of IRAS12393+3520 .

taken by M96 only 25 days after our first spectrum displays a faint,  $H_{\alpha}$  broad component, but apparently much fainter than in their low-dispersion spectrum taken about two years later. M96 noted also that the  $N_{II}/H_{\alpha}$  ratio in IRAS12393+3520 was reminiscent of a LINER (Filippenko 1993 and references therein), but that, apart of it, the spectrum was remarkably featureless. From the lack of any detectable broad component of the  $H_{\beta}$ , they estimated an amount of extinction  $E(B - V) \gtrsim 0.4$ , corresponding to  $N_H \gtrsim 2 \times 10^{21} \text{ cm}^{-2}$  (Lequeux et al. 1981; Prehdel & Schmitt 1995); such a value is not inconsistent with the reddening estimated from the narrow components. The UV spectra obtained by M96 show also broad  $Ly_{\alpha}$  and  $MgII$  emission, as well as some absorption lines. The  $E(B - V)$  inferred from the UV measurements is  $\approx 0.20$ .

The optical to X-ray Spectral Energy Distribution (SED) of IRAS12393+3520 has been studied in detail by M96. They pointed out that a scenario consisting of intense starburst can well explain the infrared, optical and UV emissions and the optical emission lines, but underestimates the soft X-rays. On the other hand, if UV and X-rays are dominated by a non-stellar contribution, the FIR emission is then highly in excess over the one typically observed in Seyfert galaxies. The presence of both sources, with comparable amount of energy output, seemed the most viable solution for this object. Secular optical variability in itself is not discriminating between the two mechanisms if timescales are not determined, as Terlevich et al. (1992) have argued that massive star formation could also account both for variability and broad lines.

IRAS12393+3520 is bright in soft X-rays [ $\log(L_{0.1-2.4\text{keV}}) = 42.80$ ], with a photon spectral index  $\Gamma \simeq 1.90$  (Moran et al. 1996). Studies in the X-rays are in principle of the uppermost importance to address

properly the true origin of the output power, because they can pierce throughout the innermost regions of the galaxy, and unveil the high-energy processes that occur in the immediate proximity of the nucleus. An ASCA observational program was started to search for evidence of nuclear activity in a sub-set of the Boller et al. (1992) soft X-ray luminous galaxies sample. In this paper, we report the results on IRAS12393+3520 (the only target for which time was allocated), which provided the first hard X-ray measure for this object. The results are presented together with a re-analysis of a pointed archival ROSAT/PSPC observation and with new optical data obtained in the mean time. We will assume  $H_0 = 50 \text{ km s}^{-1} \text{ Mpc}^{-1}$ . Energies are quoted in the source rest frame and errors are at 90% confidence level for one interesting parameter ( $\Delta\chi^2 = 2.71$ ).

## 2. X-ray Data Reduction and analysis

IRAS12393+3520 was observed by ROSAT/PSPC and ASCA on 1993, 16–17 December, and 1997, 4–5 June, respectively. The data have been retrieved from the HEASARC archive, as cleaned event lists. The ROSAT PSPC is a proportional counter sensitive in the 0.1–2 keV band, with moderate energy resolution ( $\Delta E/E \simeq 50\%$  at 1 keV) and a spatial resolution of about  $20''$  for on-axis sources. The ASCA scientific payload comprises two Solid Imaging Spectrometers (SIS0 and SIS1, sensitive in the 0.6–9 keV band, Gendreau 1995) and two Gas Imaging Spectrometers (GIS2 and GIS3, sensitive in the 0.7–10 keV band, Ohashi et al. 1996). SIS grades 0,1,2 and 4 and 1-CCD mode were used.

The best ROSAT/PSPC centroid position ( $\alpha_{2000.0} = 12^h 41^m 44^s.8$  and  $\delta_{2000.0} = 35^{\circ} 03' 46''$ ) is within  $22''$  from the optical position (Santagata et al. 1987) and  $40''$  from the ASCA centroid. The latter quantity is comparable with the typical ASCA positional uncertainties (Gotthelf & Ishibashi 1997). Several serendipitous sources are present in the PSPC field of view (see Fig. 2). Two of them could in principle contaminate the ASCA source spots. Their properties are reported in Table 1. We expect that any contamination to the IRAS12393+3520 ASCA flux is lower than 10% and 5% in the 0.5–2 and 2–10 keV bands, respectively, well within the statistical uncertainties of the ASCA measurement. PSPC scientific products have been extracted from a circular region of about  $2'$  around the apparent centroid of the source. Background spectra have been extracted in an annulus of radii  $3'20''$  and  $5'20''$ , after removing circular areas of  $2'$  radius around any serendipitous source included in the annulus.

In the SIS0 or SIS1 images no source is detected other than IRAS12393+3520, the  $3\sigma$  upper limit at the position of source #1 in PSPC field being  $8 \times 10^{-3} \text{ s}^{-1}$ . The closest serendipitous source in the GIS field of view ( $\alpha_{2000.0} = 12^h 41^m 44^s.8$  and  $\delta_{2000.0} = 35^{\circ} 03' 46''$ ; dis-

Source	$\alpha_{2000}$	$\delta_{2000}$	$N_{\text{H}}$ ( $10^{20} \text{ cm}^{-2}$ )	$\Gamma$	0.5–2 keV flux ( $10^{-14} \text{ erg cm}^{-2} \text{ s}^{-1}$ )	2–10 keV flux <sup>a</sup> ( $10^{-14} \text{ erg cm}^{-2} \text{ s}^{-1}$ )
#1	12 <sup>h</sup> 41 <sup>m</sup> 58 <sup>s</sup> .2	35°06′24″	2.0 $\pm$ 1.6	2.7 $\pm$ 0.5	5	6
#2	12 <sup>h</sup> 41 <sup>m</sup> 58 <sup>s</sup> .8	35°03′21″	< 1.2	2.2 $\pm$ 0.8	1.7	1.5

<sup>a</sup>extrapolated from the best-fit PSPC model

**Table 1.** Properties of the serendipitous sources #1 and #2 in the PSPC field. Spectra parameters refer to a power-law plus photoelectric absorption model of the PSPC spectrum.

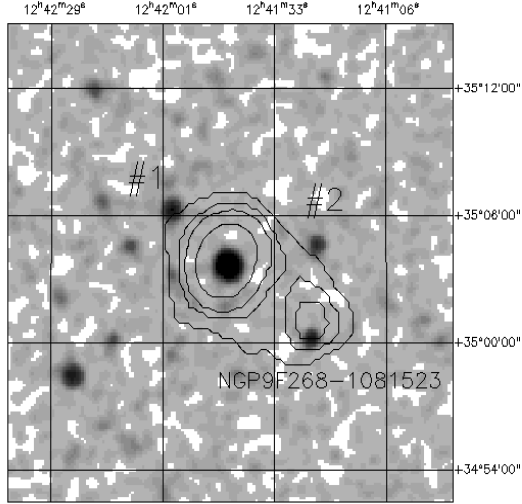


**Fig. 2.** PSPC field of view of IRAS12393+3520 (the central source) superimposed to the GIS2 intensity contours of the ASCA observation

tance 5.8′) is probably associated with the foreground galaxy NGP9 F268-1081523. ASCA source scientific products have been then extracted from circles of radii 4′, 3′.25 and 3′.75, in the SIS0, SIS1 and GIS, respectively. Background scientific products have been extracted from regions of the field of view free from contaminating sources. None of the presented results changes significantly if the background is extracted from blank sky fields. Total exposure times are about 33, 32 and 13 ks for the SIS, GIS and PSPC, respectively. Full band count rates were  $(3.79 \pm 0.12)$ ,  $(2.77 \pm 0.11)$ ,  $(1.89 \pm 0.09)$ ,  $(2.38 \pm 0.10)$  and  $(6.4 \pm 0.3) \times 10^{-2} \text{ s}^{-1}$ , for the SIS0, SIS1, GIS2, GIS3 and PSPC, respectively.

### 2.1. The X-ray light curve

In Fig. 3 the light curves in the 0.1–2 keV (PSPC) and 0.5–4 keV bands (SIS) are shown. The latter shows a gentle rise and decay before about 50 ks from the start of the observation. A similar trend is observed in the GIS light curves. If a fit with a constant line is performed on the light curve,  $\chi^2|_{\text{ASCA}} = 30/15$  degrees of freedom (dof). From the flux change rate of the light curve in the 5–35 and 35–50 ks

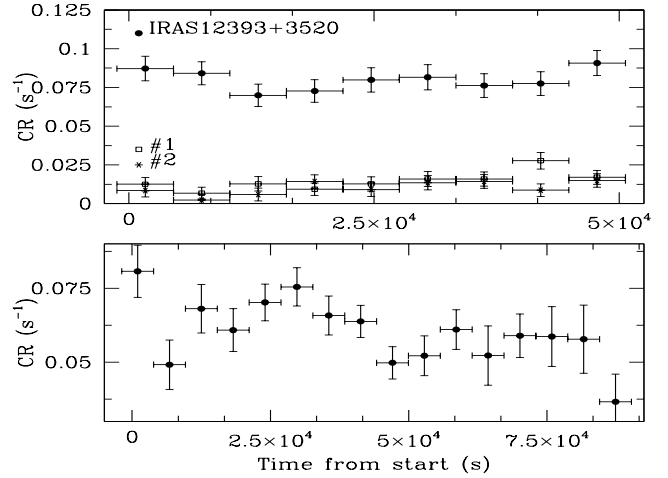


**Fig. 3.** 0.1–2 keV background-subtracted (ROSAT/PSPC, *upper panel*) and 0.5–4 keV (ASCA/SIS, *lower panel*) light curves. Binning time is 5760 s. Only bins with an exposure fraction higher than 15% are shown. If a linear fit is performed on the ASCA light curve in the 5–35 and 35–50 ks intervals, one obtains a rate of flux change of  $40 \pm 30\%$  and  $40 \pm 20\%$ , respectively

intervals, we estimate a minimum doubling/halving time in the range 30–75 ks. Variability on lower timescales cannot be ruled out, but the limited available statistics prevented us to reach a firm conclusion on its existence. This variability is not associated with any of the serendipitous sources detected in the PSPC and laying at the border of the ASCA extraction regions. We have extracted SIS0 images in the time intervals between 10–40 and 50–80 ks after the beginning of the ASCA observation. The source spot does not show sign of elongation and the centroid best-fit positions agree within 6″. Although an eye inspection of the PSPC light curve might suggest that a similar variability was observed by ROSAT as well, the evidence is not statistically that clear ( $\chi^2|_{\text{ROSAT}} = 18/21$  dof). We have searched for spectral dynamics associated with the ASCA flux changes, without success. We will therefore focus in the next section on the time averaged spectrum of IRAS12393+3520.

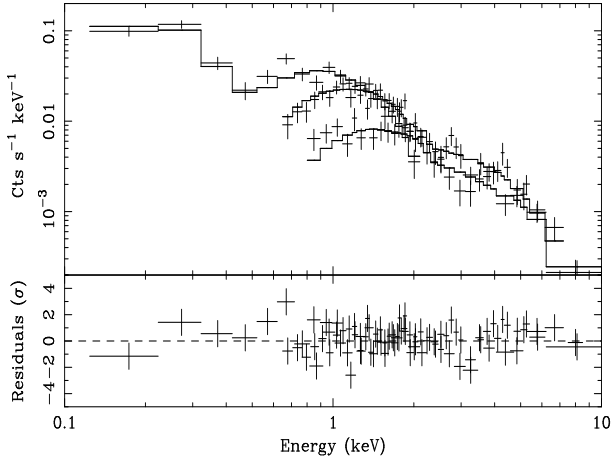


**Fig. 4.** PSPC, SIS0 and GIS2 spectra (*upper panel*) and residuals in units of standard deviations (*lower panel*) when a photoelectric absorbed power-law model is applied to the data of all detector simultaneously. Each data point has a signal-to-noise ratio  $> 3$

## 2.2. Spectral analysis

All spectra have been rebinned in order to have at least 20 counts per energy channel, in order to ensure the applicability of the  $\chi^2$  statistics. Proper matrices for the date of the observations have been retrieved from the HEASARC archive or built with the software available in the FTOOLS 4.0 version. First, we fitted the PSPC and ASCA spectra in the overlapping 0.8–2 keV band with a simple photoelectric absorbed power-law model, leaving all parameters free (except the  $N_{\text{H}}$ , which has been tight to be the same for all instruments), to check if significant spectral variability arose between the epochs of the two observations. The spectral indices turn out to be well consistent within the statistical uncertainties ( $\Gamma_{\text{ROSAT}}^{0.8-2\text{keV}} = 1.7 \pm 1.0$ ;  $\Gamma_{\text{ASCA}}^{0.8-2\text{keV}} = 1.5 \pm 0.7$ ), despite of an increase in the flux of  $\simeq 130\%$ . In the following, we will therefore fit the spectra of all detectors simultaneously, only allowing a relative normalization factor as a free parameter among all the instruments.

In Fig. 4, the results of a spectral fit with a simple power-law with photoelectric absorption are shown. The fit is rather good ( $\chi^2 = 188/177$  dof), with  $\Gamma = 1.55 \pm 0.08$  and  $N_{\text{H}} = (0.8 \pm 0.3) \times 10^{20} \text{ cm}^{-2}$ . Further spectral complexity is not strongly required by the data. The only feature, whose addition is required at  $\simeq 99\%$  level, is an absorption edge ( $\Delta\chi^2 = 9$  for two more parameters), with threshold energy  $E_{\text{th}} = 0.71 \pm 0.06$ , formally consistent with the K-shell photoionization energy of OVII. The edge is detected with comparable significance in both the ROSAT and ASCA spectra separately. Similar features have been commonly observed in the spectra of Seyfert 1 galaxies (Reynolds 1997; George et al. 1998). The addition of this feature makes the spectrum steeper and therefore

consistent with that typically observed in Seyfert 1 galaxies (Nandra & Pounds 1994; Nandra et al. 1997b; see Table 2). We have therefore performed a fit with a Seyfert-like model, constituted by a Compton-reflected power-law (model `pexrav` in XSPEC, Magdziarz & Zdziarski 1995), an absorption edge and a fluorescent broad (i.e.:  $\sigma = 0.43$  keV, Nandra et al. 1997b) iron line from neutral iron (i.e.: centroid energy held fixed to 6.4 keV). The line is actually not required by the fit, but we have included it because it is expected on theoretical grounds (George & Fabian 1991; Matt et al. 1992). The fit is comparably good as in the simple power-law case. The amount of reflection, parameterized through the ratio between the reflected and the transmitted components,  $R^1$ , is  $> 1.3$ , which is not inconsistent with the upper limit on the EW of the iron line (600 eV), if standard cosmic abundances are assumed (Matt et al. 1992). If we add to this model a 1 keV thermal emission from an optically thin plasma, its 0.1–10 keV luminosity is constrained to be lower than  $3.8 \times 10^{41} \text{ erg s}^{-1}$  at the 90% confidence level. The cold absorbing column density is broadly consistent with the Galactic contribution along the IRAS12393+3520 line of sight ( $N_{\text{H,Gal}} = 1.4 \times 10^{20} \text{ cm}^{-2}$ , Dickey & Lockman 1990). The fluxes in the 0.5–2, 0.5–4.5 and 2–10 keV energy bands are  $5.2 \times 10^{-13}$ , 1.00 and  $1.12 \times 10^{-12} \text{ erg cm}^{-2} \text{ s}^{-1}$ , implying rest frame unabsorbed luminosities of 1.29, 2.4 and  $2.6 \times 10^{42} \text{ erg s}^{-1}$ , respectively.

Alternatively, a good fit can be formally obtained also with a double-temperature optically thin plasma (code `mekal` in XSPEC), with temperatures  $\simeq 100$  eV and  $\simeq 8$  keV and abundances consistent with solar. In this scenario, the contribution of a  $\Gamma = 1.9$  (1.0) power-law to the 0.5–4 keV flux is lower than 7% (6%).

## 3. Additional optical data

An intermediate resolution spectrum (1.8 Å per pixel) of the  $H_{\alpha}$  region of NGC 4619 was obtained in January 1996 at OHP. The calibrated one dimensional spectrum has been extracted in two ways, shown in Fig. 5. The first one (upper spectrum in Fig. 5) integrates over all the length where  $H_{\alpha}$  is detected (about 40''): the emission lines are clearly detected, with a  $[\text{NII}]/H_{\alpha}$  ratio stronger than in standard HII regions. This ratio was the basis for the LINER claim in M96. Unfortunately, the  $[\text{SII}]$  lines, which could provide an additional diagnostic, fall into an atmospheric absorption line. As any clear broad component, revealing an AGN, could be hidden in a much larger star forming region, a second extraction was performed over a

<sup>1</sup>  $R$  is equal to 1 when the reflection occurs in a plane-parallel infinite slab. A higher value might imply either a higher solid angle subtended by the disk to the source - as e.g. in a disk “warped” geometry -, a delay in the disk response to flux changes of the primary continuum, or an anisotropy of the nuclear emission, such that the disk sees more flux than emitted along our cone-of-sight

Model	$N_{\text{H}}$ ( $10^{20} \text{ cm}^{-2}$ )	$\Gamma$	R	$E_{\text{th}}$ (keV)	$\tau$	$\chi^2/\text{dof}$
wa*ed*(px+ga)	$1.6 \pm_{0.4}^{0.5}$	$1.78 \pm_{0.11}^{0.12}$	0 <sup>†</sup>	$0.71 \pm_{0.06}^{0.05}$	$0.7 \pm_{0.3}^{0.4}$	172.4/175
wa*ed*(px+ga)	$1.7 \pm_{0.4}^{0.5}$	$1.82 \pm_{0.11}^{0.12}$	1 <sup>†</sup>	$0.71 \pm_{0.06}^{0.04}$	$0.8 \pm 0.4$	171.0/175
wa*ed*(px+ga)	$2.3 \pm_{0.7}^{1.0}$	$2.0 \pm_{0.2}^{0.3}$	$7.0 \pm_{5.7}^{9.0}$	$0.69 \pm_{0.04}^{0.05}$	$1.0 \pm_{0.4}^{0.5}$	167.7/174
Model	$N_{\text{H}}$ ( $10^{20} \text{ cm}^{-2}$ )	$kT_1$ (eV)	$kT_2$ (keV)	$Z_1 = Z_2$ %	$\chi^2/\text{dof}$	
wa*(mk+mk+ga)	$3.1 \pm 1.8$	$110 \pm 40$	$8.1 \pm_{1.6}^{2.5}$	$0.6 \pm_{0.4}^{0.5}$	181.4/175	

<sup>†</sup>fixed

**Table 2.** Best-fit parameters and results. *wa* = photoelectric absorption; *ed* = photoelectric absorption edge; *px* = Compton reflection; *mk* = optically thin plasma; *ga* = Gaussian emission line

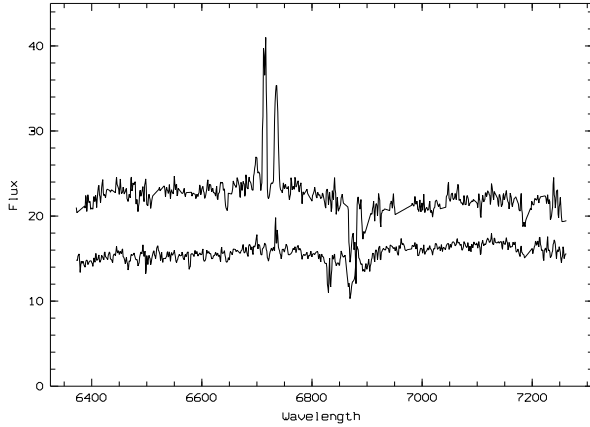


**Fig. 5.** January 1996 IRAS12393+3520 high dispersion spectra, with extraction integrated along 40'' (*upper*) and 10'' (*lower*) slit lengths.

smaller extension (about 10''), corresponding to the strong continuum. This is the lower spectrum of Fig. 5, where only weak [NII] emission lines are seen, and almost no  $H_{\alpha}$ . As the latter may however be hidden in the corresponding stellar absorption, it is difficult to use the [NII]/ $H_{\alpha}$  line ratio alone to claim for a diagnostic of Seyfert or LINER. In both spectra a broad  $H_{\alpha}$  component may be marginally seen but, if present, is certainly not as strong as seen in the high dispersion spectrum of M96 (and even less so than in their low dispersion one).

We finally obtained a new, low dispersion spectrum, in June 1999 at OHP, and the result is shown in Fig. 6. This spectrum, extracted over a similar 10'' width as the lower one in Fig. 5, shows a clear, broad, asymmetric wing to  $H_{\alpha}$ , with a strong component on the blue side (where nothing was suspected in our 1992 spectrum) very similar to the one seen in the low dispersion spectra of M96 and Moran et al. (1994). While a quantitative comparison between the various spectra is difficult, as slit orientations and extraction lengths are different (and not always well documented), we have here reasonable evidence for

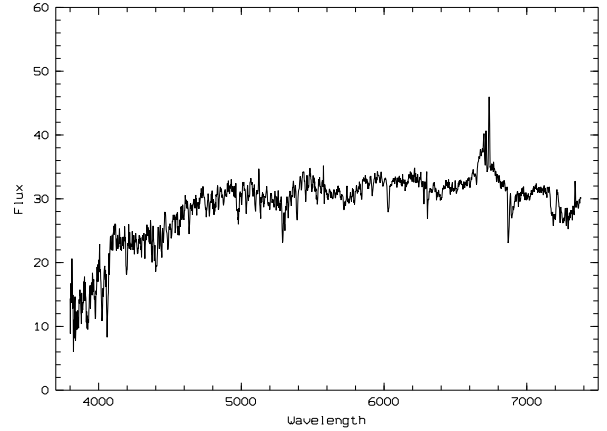


**Fig. 6.** June 1999 low dispersion spectrum of IRAS12393+3520.

variations of a broad-line component in a spectrum otherwise dominated by intermediate-type stars. The broad  $H_{\alpha}$  component is absent or weak in the first available spectra (ours in March 1992, the high-resolution one of April 1992 in M96), is strong in the low dispersion spectra of Moran et al. (1994) and of M96 (July 1994), dimmed again in our data of January 1996 and strong again in our last spectrum in June 1999. The variations seen are between a Seyfert 1.9 spectrum and a spectrum dominated by stellar features. Some indications exist for a LINER identification: we see a strong [NII]/ $H_{\alpha}$  ratio, as M96 did, and our 1999 spectrum shows also an [OII]/[OIII] ratio much greater than one. We have however no detection of the [OI] line with a strength which could confirm the LINER diagnostic (Heckman, 1980). We note that up to now, only one case is known where broad lines developed in a LINER (NGC 1097; Storchi-Bergmann et al. 1993). The substantial reddening derived in our last spectrum [ $E(B - V) \simeq 0.8 - 0.9$ , consistent between the Balmer decrement in the narrow component and the NaD absorption], is certainly an element of importance in the following discussion.

## 4. Discussion

### 4.1. The hard X-ray properties of IRAS12393+3520

X-rays provide a strong evidence in favor of the existence of an AGN in IRAS12393+3520. We have detected a significant variability of the X-ray light curve. The minimum observed associated doubling/halving time is comprised in the range 30–75 ks. If the variability is intrinsic to the radiation emitted in the nuclear region of an AGN, usual light crossing arguments constrain the mass of the nuclear black hole to be  $< 10^9 \eta_5^{-1} M_\odot$ , where  $\eta_5 \equiv r/(5R_S)$  is the typical size of the region emitting the bulk of the primary non-thermal continuum in unit of five Schwarzschild radii. The joint ROSAT/ASCA 0.1–10 keV spectrum has also a shape which closely resembles the one typically observed in radio-quiet AGN. Our data suggest that the solid angle subtended by the accretion disk is higher than due to a plane-parallel infinite slab. The upper limit on the EW of a fluorescent neutral iron line (600 eV) is not inconsistent with this scenario if solar abundances are assumed. However, much better quality of the data is required to confirm this hint.

The data require at 99% level of confidence the presence of an absorption edge, whose threshold energy is consistent with the K-shell photoionization energy of OVII. In at least 50% of Seyfert 1s the nuclear radiation is absorbed by substantially ionized matter (Reynolds 1997; George et al. 1998). In IRAS12393+3520 the properties of the absorbing matter are statistically poorly constrained and are somewhat dependent on the assumed continuum model. We conservatively derive a column density in the range  $2.5\text{--}7.5 \times 10^{21} \text{ cm}^{-2}$  [or  $E(B - V) \simeq 0.5\text{--}1.5$  under standard assumptions], if the physical conditions required to sustain an oxygen state dominated by He-like are assumed. If the warm absorber contains dust in the Galactic dust-to-gas ratio, such a medium may account for the observed optical reddening and explain the missing  $H_\beta$  broad line, even in the presence of a strong broad  $H_\alpha$  (which is actually detected only in some of the IRAS12393+3520 optical spectra, cf. Sect. 3). “Dusty” warm absorbers have already been invoked to explain the discrepancy between the amount of X-ray cold absorption and the optical reddening in a few Seyfert galaxies (Reynolds et al. 1997; Komossa & Fink 1998 and references therein), although Siebert et al. (1999) have recently shown that such a “simple” representation was not able to reproduce all the observed optical and X-rays data in the case of a well studied example, IRAS13349+2438.

The observed spectra can be formally accounted by a two-temperature optically thin plasma, in analogy with recent evidence on the X-ray emission of starburst galaxies (Della Ceca et al. 1998; Cappi et al. 1999). In this scenario, however, the observed short-term variability cannot be explained, unless it represents the diluted appearance of a much more variable underlying unresolved source. The lack of spectral variability during the ASCA observation

points against the emerging of a further source in the spectrum in correspondence to the flux variation. The contribution of a power-law source in the 0.5–4 keV band is constrained to be lower than  $1.8 \times 10^{41} \text{ erg s}^{-1}$ . To reproduce the observed flux change, it should vary in  $10^4$  seconds by an amount  $\simeq \frac{12}{L_{41}}$ , where  $L_{41}$  is the X-ray luminosity in units of  $10^{41} \text{ erg s}^{-1}$ . This rules out the possible serendipitous detection of local X-ray binaries or superluminous sources; the latter ones exhibit indeed variability in flux by an amount up to two orders of magnitude, but have normally luminosities well within  $10^{39} \text{ erg s}^{-1}$ . On the other hand, X-ray variability on such timescales is rather common in Seyfert galaxies (Nandra et al. 1997a and references therein). The timescales are too fast to be explained by mechanisms which do not invoke accretion on a supermassive black hole (*e.g.* the starburst model of Terlevich et al. 1992).

### 4.2. Comparison between X-ray and other wavelengths

An energetic argument points against the idea that hard X-rays are dominated by a nuclear starburst. No known starburst galaxy is so X-ray luminous (Ptak et al. 1999). The soft-X vs.  $60\mu\text{m}$  and soft-X vs. UV luminosity ratios are  $1.9 \times 10^{-2}$  and  $1.2 \times 10^{-2}$ , more than one order of magnitude higher than typical values observed in star forming galaxies (SFG, Mass-Hesse et al. 1995). The observed X-ray luminosity  $\sim 4 \times 10^{42} \text{ erg s}^{-1}$  is, on the other hand, not uncommon among Seyfert galaxies. In Figure 7 the IRAS12393+3520 SED is shown, superimposed to the average “tracks” of the Mass-Hesse et al. (1995) sample for Seyfert 1s, Seyfert 2s, QSO and SFG. Caution must be employed when evaluating the SED in IRAS12393+3520, because it refers to non-simultaneous measurements. Optical spectroscopy suggests that the nuclear activity (as seen by the BLR), and therefore also the energy budget, might be variable with time. Given these caveats, one notes that IRAS12393+3520 follows apparently better a Seyfert 2 SED (or eventually a SFG one), being strongly under-luminous in UV and X-rays in comparison to the IR, if the normalization is done in the far-IR. These pieces of information are summarized in the IR, UV and X-ray color-color plot of Figure 8, where IRAS12393+3520 is seen to lie in the region of Seyfert galaxies, and apparently type 2 rather than 1. The X vs. [OIII] luminosity ratio is  $3.7 \times 10^2$ , an order of magnitude greater than observed in Seyfert 1s (cf. Fig. 6 in Maiolino et al. 1998) and would also point towards a Seyfert 2 identification.

Several pieces of evidence point, however, against an identification of IRAS12393+3520 as a Seyfert 2. First, there is no evidence of the high excitation typical of Sey2’s: the [OIII] over  $H_\beta$  line ratio is difficult to measure accurately, as [OIII] is faint and  $H_\beta$  is hidden in the corresponding stellar absorption, but is not larger than three. In addition, the [OII]/[OIII] ratio is much larger than one, and it is the combination of these line ratios, with the

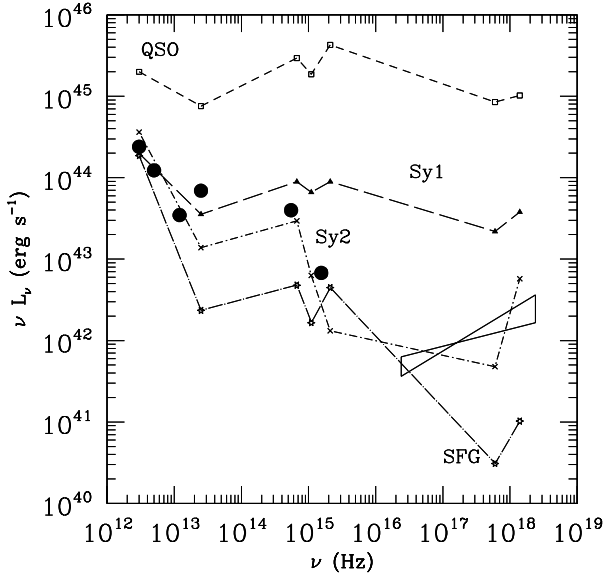


**Fig. 7.** IRAS12393+3520 SED (filled circles and bowtie) compared with the average “tracks” observed in quasars (QSO, empty squares), Seyfert 1s (Sy1, filled triangles), Seyfert 2s (Sy2, crosses) and star forming galaxies (SFG, empty stars; Mass-Hesse et al. 1995). IR to UV IRAS12393+3520 photometry points are from M96.

[NII]/ $H_\alpha$  one, which lead to the LINER claim for this object. This is not compatible with a Seyfert 2 identification. Moreover, a high excitation is not seen either when the broad  $H_\alpha$  component is absent, so that the variations cannot be described as a transition between a Seyfert 1 and a Seyfert 2 phase, as seen in some other cases (e.g. Mkn 993, Tran et al. 1992; Mkn 6, Khachikian & Weedman 1971; Mkn 1018, Cohen et al. 1986). Second, the X-ray intrinsic neutral absorption column density is negligible. No model where the nuclear power-law is strongly absorbed yields comparably good fits to the ROSAT/ASCA spectrum as the simple models of Table 2, even if one allows the covering fraction of the absorbing matter to be lower than 1. One might suppose that the X-ray spectrum is totally dominated by scattered radiation from an otherwise invisible nucleus, as observed in several “reflection-dominated” Seyfert 2s (Turner et al. 1997; Matt et al. 1997; Guainazzi et al. 1999). The observed variability, however, introduces severe constraints on this possibility. Assuming a typical variability timescale of  $\Delta t \approx 4 \times 10^4$  s, light crossing arguments imply a lower limit on the electron numerical density  $n_e \gtrsim (c\Delta t\sigma_{sc})^{-1} \sim 1.2 \times 10^9 \text{ cm}^{-3}$ . If the absorption occurs in the same medium, an optical depth to scattering of the order of one implies an optical path  $\sim N_H/n_e \lesssim 4 \times 10^{12}$  cm. Such a low value would imply that the scattering/absorption occurs in the proximity of the galactic nucleus, hardly compatible with the idea that the matter hiding the nuclear region is located at dis-

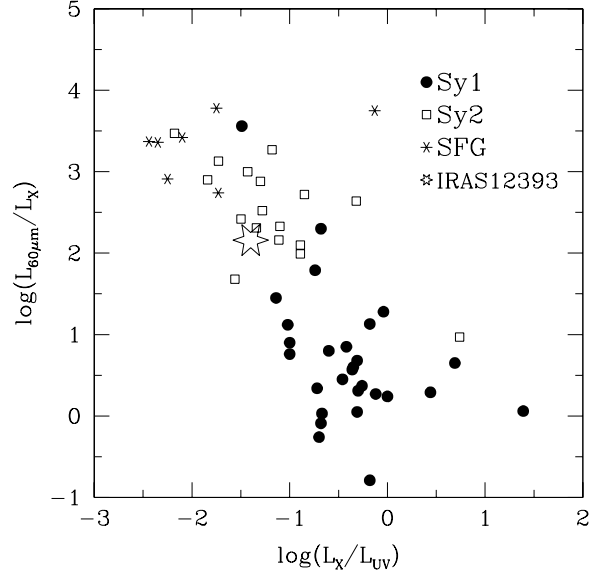


**Fig. 8.** IR (60  $\mu\text{m}$ ), UV (2700  $\text{\AA}$ ) and X-ray (0.5–4.5 keV) color-color diagram for Seyfert 1s (filled circles), Seyfert 1.5–2 (empty squares) and SFG (stars). The location of IRAS12393+3520 is indicated by the big empty star. Data are from Mass-Hesse et al. 1995

tances  $\sim 1$ –100 pc, in the shape of a, more or less homogeneous, azimuthally symmetric structure (Antonucci & Miller 1985; Maiolino & Rielke 1995; Greenhill et al. 1996). Finally, the appearance sometimes of a broad  $H_\alpha$  component is a definite sign in favor of a Seyfert 1 classification.

One clue to explain the observed SED is to assume that the AGN is a weak Seyfert 1, which is over-luminous in IR in comparison to the objects of the same class of comparable X-ray luminosity. This interpretation can be naturally linked to the puzzling absorption pattern emerging from the optical/UV spectroscopy. Very broad  $\text{Ly}\alpha$  and  $H_\alpha$  lines have been observed in (not simultaneous) observations of the core of IRAS12393+3520 (M96). All these evidences suggest that the geometrical distribution of the circumnuclear neutral absorbing matter is far more complex than the simple equatorially symmetric pattern, which is assumed in the 0-th order Seyfert unification theories (Antonucci & Miller 1985; Antonucci 1993). The Narrow Line Region (NLR) could be absorbed by dusty, optically thick matter distributed on spatial scale of a few hundreds of parsec, which does not (not always?) intercept the line of sight towards the nuclear environment. This dust might simultaneously be responsible for the IR emission through reprocessing of the incoming nuclear radiation during particularly active phases (or when the line of sight between the nucleus and the dust is unobscured). In the same framework, the under-luminosity in  $L_{[\text{OIII}]}$  and the relative over-luminosity in IR in comparison to the

directly observed X-ray of nuclear origin can be simultaneously explained. A similar scenario had been originally suggested by Maiolino & Rieke (1995), who proposed that “intermediate” Seyfert galaxies are seen through a 100 pc-scale torus coplanar with the plane of the galaxies. This idea has received a further support after the results of a recent HST slew survey, which lead to the discovery that the distribution of matter in the nuclear environment of radio-quiet, nearby AGN is indeed highly patchy, with dusty lanes protruding from several kilo-parsecs to a few hundreds of parsecs towards the center (Malkan et al. 1998). Recently, Maiolino et al. (1999) pointed out that barred galaxies (like IRAS12393+3520) tend to exhibit the highest values of IR to X-ray luminosity ratio (see, however, a different point of view in Regan & Mulchaey (1999)). This might suggest that stellar bars are very efficient in driving gas to the circumnuclear region and therefore to provide high amount of warm (AGN-heated) dust in the nuclear environment, which would reprocess the nuclear high-energy continuum.

The bulk of the IR radiation could alternatively be produced by an intense star formation episode, occurring on spatial scales of the order or larger than the NLR. The SED in the IR alone is typical of starburst galaxies and does not satisfy the various criteria defined to select AGN in IRAS data (de Grijp et al. 1985; Désert & Dennefeld 1988). Also, the standard IR/radio parameter  $q$ , discussed by Condon et al. (1995), has a value of 2.85 for IRAS12393+3520, showing that the AGN, if present, is not dominating the IR emission and/or that the object is radio-weak. Finally, the observed infrared luminosity ( $L_{\text{IR}} \sim 5 \times 10^{44} \text{ erg s}^{-1}$ ; M96) is almost two orders of magnitude higher than expected from the AGN 1–10 keV luminosity ( $L_{\text{X}} \sim 3 \times 10^{42} \text{ erg s}^{-1}$ ), if the IRAS12393+3520 AGN SED has a  $L_{\text{IR}}/L_{\text{X}}$  ratio typical for quasars with  $L_{\text{X}} < 10^{45} \text{ erg s}^{-1}$  ( $\simeq 4.5$ ; Elvis et al. 1994).

While both explanations for the IR emission are plausible, the energetic argument just discussed favors the hypothesis that the IR emission is dominated by star-formation. However, even in this case, an additional (nuclear) source of high-energy radiation is required to explain the hard X-rays. As shown in Fig. 8, IRAS12393+3520 exhibits indeed a much higher X-ray to IR or UV luminosity flux than typically observed in SFG galaxies. It is likely to be provided by a separate component, which is straightforward to identify, in the light of the ASCA/ROSAT results, with an active nucleus. On the other hand, a spatially and physically structured and time varying absorber is also required to yield the observed different absorptions towards the nucleus, of the BLR and of the NLR lines. The dusty environment of a star forming region could provide only the last. IRAS12393+3520 is therefore best described by a central, weak, AGN, with a BLR partly obscured by a structured absorber, and a well absorbed NLR, mixed with a region of intense star formation of perhaps larger extension.

*Acknowledgements.* MG acknowledges the receipt of an ESA Research Fellowship. The authors acknowledge discussions with F.Bocchino. This research has made use of the NASA/IPAC Extragalactic Database, which is operated by the Jet Propulsion Laboratory under contract with NASA, and of data obtained through the High Energy Astrophysics Science Archive Research Center Online Service, provided by the NASA/Goddard Space Flight Center.

## References

- Antonucci R.R.J., 1993, ARAA 31, 473  
 Antonucci R.R.J., Miller J.S., 1985, ApJ 297, 621  
 Boller T., Meurs E.J.A., Brinkmann W., et al., 1992, A&A 261, 57  
 Boller T., Dennefeld M., Brinkmann W., Fink H. and Meurs E.J.A., 1993 in “First light in the Universe: Stars or QSOs?”, Editions Frontières, Rocca-Volmerange B., Guiderdoni B., Dennefeld M., Tran Thanh Van J. (eds.), p.339  
 Cappi M., Persic M., Bassani L., et al., 1999, A&A 350, 777  
 Cohen R.D., Puetter R.C., Rudy R.J., Ake T.B., Foltz C.B., 1986, ApJ 311, 135  
 Condon J.J., Andreson E., Broderick J.J., 1995, AJ 109, 2318  
 Della Ceca R., Griffiths R.E., Heckman T.M., Lehnert M.D., Weaver K. A., 1998, ApJ 514, 772  
 Désert F.X.D., Dennefeld M., 1988, A&A 206, 227  
 Dickey J.M., Lockman F.J., 1990, ARAA 28, 215  
 Elvis M., Wilkes B., McDowell J.C., et al., 1994, ApJS 95, 1  
 Filippenko A.V., 1993, in “The nearest active galaxies”, Beckman L., Colina L. and Netzer H. (eds.), Consejo Superior de Investigaciones Científicas, Madrid, p.99  
 Gendreau K., 1995, Ph.D. thesis, Massachusetts Institute of Technology  
 George I.M., Fabian A.C., 1991, MNRAS 249, 352  
 George I.M., Turner T.J., Netzer H., et al., 1998, ApJS 114, 73  
 de Grijp M.H.K., Miley G.K., Lub J., de Jong T., 1985, Nat 314, 240  
 Gotthelf E.V., Ishibashi K., 1997, in “X-ray Imaging and Spectroscopy of Cosmic Hot Plasma”, Makino F., Mitsuda K. (eds.) (Tokyo:Universal Academy Press), 631  
 Greenhill L.J., Grainer C.R., Antonucci R., Barvanis R., 1996, ApJ 472, L21  
 Guainazzi M., Matt G., Antonelli L.A., et al. 1999, MNRAS, 310, 10  
 Heckman T.M., 1980, A&A 87, 152  
 Khachikian E.Y., Weedman D.W., 1971, ApJ 164, L109  
 Komossa S., Fink H.H., 1998, in Proceedings of “Highlights in X-ray Astronomy”, Aschenbach B. et al. (eds.), in press (astroph/9808205)  
 Lequeux J., Maucherat-Joubert M., Deharveng J.M., Kunth D., 1981, A&A, 103, 305  
 Magdziarz P., Zdziarski A.A., 1995, MNRAS 273, 837  
 Maiolino R., Rieke G.H., 1995, ApJ 454, 95  
 Maiolino R., Salvati M., Bassani L., et al., 1998, A&A 338, 781  
 Maiolino R., Risaliti G., Salvati M., 1999, A&A 341, 35  
 Malkan M.A., Varoujan G., Tam R., 1998, ApJS 94, 517  
 Mas-Hesse J.M., Rodríguez-Pascal P.M., de Cordoba L.S.F., et al., 1995, A&A 298, 22  
 Mas-Hesse J.M., Cerviño M., Rodríguez-Pascal P.M., Boller T., 1996, A&A 309, 431 (M96)



- Matt G., Perola G.C., Piro L., Stella L., 1992, *A&A* 257, 63
- Matt G., Guainazzi M., Frontera F., et al., 1997, *A&A* 325, L13
- Moran E.C., Halpern J.P., Helfand D.J., 1994, *ApJ* 433, L65
- Moran E.C., Halpern J.P., Helfand D.J., 1996, *ApJS* 106, 341
- Nandra K., Pounds K.A., 1994, *MNRAS* 268, 405
- Nandra K., George I.M., Mushotzky R.F., Turner T.J., Yaqoob Y., 1997a, *ApJ* 476, 70
- Nandra K., George I.M., Mushotzky R.F., Turner T.J., Yaqoob Y., 1997b, *ApJ* 477, 602
- Ohashi T., Ebisawa K., Fukazawa Y., et al., 1996 *PASJ* 48, 157
- Prehdel P., Schmitt J.H.M.M., 1995, *A&A* 293, 889
- Ptak A., Serlemitsos R., Yaqoob T., Mushotzky R., 1999, *ApJS* 120, 179
- Regan M.W., Mulchaey J.S., 1999, *AJ*, 117, 2676
- Reynolds C.S., 1997, *MNRAS* 286, 513
- Reynolds C.S., Ward M.J., Fabian A.C., Celotti A., 1997, *MNRAS* 291, 403
- Santagata N., Basso L., Gottardi L., et al., 1987, *A&AS* 70, 191
- Siebert J., Komossa S., Brinkmann W., 1999, *A&A*, 351, 893
- Storchi-Bergmann Th., Baldwin J.A., Wilson A.S., 1993, *ApJ* 410, L11
- Terlevich R., Tenorio-Tagle G., Franco J., Melnick J., 1992, *MNRAS* 255, 713
- Tran H.D., Osterbrock D.E., Martel A., 1992, *A.J.* 104, 2072
- Turner T.J., George I.M., Nandra K., Mushotzky R.F., 1997, *ApJS* 113, 23